Environmental Science & Technology

pubs.acs.org/est

Article

Inducing Inorganic Carbon Accrual in Subsoil through Biochar Application on Calcareous Topsoil

Yang Wang, Stephen Joseph, Xiang Wang, Zhe H. Weng, David R.G. Mitchell, Mitchell Nancarrow, Sarasadat Taherymoosavi, Paul Munroe, Guitong Li, Qimei Lin, Qing Chen, Markus Flury, Annette Cowie, Olivier Husson, Lukas Van Zwieten, Yakov Kuzyakov, Johannes Lehmann, Baoguo Li, and Jianying Shang*

Cite This: *Environ. Sci. Technol.* 2023, 57, 1837−1847

Read Online

ACCESS | Metrics & More | Article Recommendations | Supporting Information

ABSTRACT: Biochar amendments add persistent organic carbon to soil and can stabilize rhizodeposits and existing soil organic carbon (SOC), but effects of biochar on subsoil carbon stocks have been overlooked. We quantified changes in soil inorganic carbon (SIC) and SOC to 2 m depth 10 years after biochar application to calcareous soil. The total soil carbon (i.e., existing SOC, SIC, and biochar-C) increased by 71, 182, and 210% for B30, B60, and B90, respectively. Biochar application at 30, 60, and 90 t ha^{-1} rates significantly increased SIC by 10, 38, and 68 t ha^{-1}, respectively, with accumulation mainly occurring in the subsoil (below 1 m). This huge increase of SIC (mainly $CaCO_3$) is ∼100 times larger than the inorganic carbon present in the added biochar (0.3, 0.6, or 0.9 t ha^{-1}). The benzene polycarboxylic acid method showed that the biochar-amended soil contained more black carbon particles (6.8 times higher than control soil) in the depth of 1.4−1.6 m, which provided the direct quantitative evidence for biochar migration into subsoil after a decade. Spectral and energy spectrum analysis also showed an obvious biochar structure in the biochar-amended subsoil, accompanied by a Ca/Mg carbonate cluster, which provided further evidence for downward migration of biochar after a decade. To explain SIC accumulation in subsoil with biochar amendment, the interacting mechanisms are proposed: (1) biochar amendment significantly increases subsoil pH (0.3−0.5 units) 10 years after biochar application, thus forming a favorable pH environment in the subsoil to precipitate HCO_3^-; and (2) the transported biochar in subsoil can act as nuclei to precipitate SIC. Biochar amendment enhanced SIC by up to 80%; thus, the effects on carbon stocks in subsoil must be understood to inform strategies for carbon dioxide removal through biochar application. Our study provided critical knowledge on the impact of biochar application to topsoil on carbon stocks in subsoil in the long term.

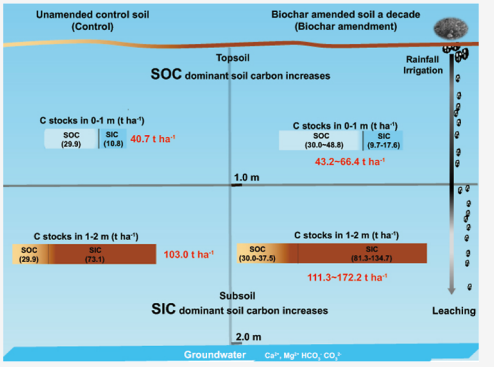

KEYWORDS: *biochar, transport, soil inorganic carbon, subsoil, soil pH, nuclei, geochemistry carbon cycling, climate change*

INTRODUCTION

Atmospheric carbon dioxide (CO_2) and other greenhouse gas levels continue to increase, constraining the world's capacity to meet the Paris Agreement goal of limiting warming below 2 degrees Celsius.[1−3] The Intergovernmental Panel on Climate Change has identified soil carbon management[4,5] and biochar application[6] as carbon dioxide removal techniques that can contribute to achieving that goal. Biochar addition to soils sequesters carbon (C) as persistent organic carbon (OC)[7,8] and can further contribute to climate change mitigation through stabilization of rhizodeposits and existing soil organic carbon (SOC),[9] reduce greenhouse gas emissions from soil,[10,11] increase plant growth,[12,13] and displacement of greenhouse gas emissions from fossil fuels.[6] However, the effects of biochar on soil inorganic carbon (SIC) in subsoil (below 1 m) have not been studied in detail.

SIC is an important carbon form, and its stocks in arid and semi-arid regions are much larger than the corresponding SOC stocks.[14] The SIC dynamics in the pedosphere include the weathering of carbonate and silicate rocks,[15] and the formation and dissolution of pedogenic inorganic carbonates.[16] Increasing SIC constitutes direct carbon dioxide removal, and strategies to increase SIC on land include accelerating silicate rock weathering[17,18] and using crushed rock waste in mines.[19] Biochar is generally recommended as a technology for the sequestration of organic carbon. However, researchers have

Received: September 3, 2022
Revised: November 22, 2022
Accepted: December 15, 2022
Published: January 3, 2023

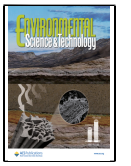

https://doi.org/10.1021/acs.est.2c06419
Environ. Sci. Technol. 2023, 57, 1837−1847

recently found that biochar application increased the SIC stocks in topsoil.[20−22] The few studies that have examined biochar effects on SIC have found distinct results in different soil depths, with increases at soil depths of 0−0.3 m,[20,21] and reduction at a sampling depth of 0−1 m.[22] However, most of the SIC is distributed in the subsoil deeper than 1 m. The long-term effects of biochar application on subsoil carbon stocks, especially inorganic carbon stocks, are not well-studied. The related knowledge is lacking from field experiments to verify the response of subsoil to biochar amendments in topsoil in the long term. This is a critical knowledge gap in assessing the impact of biochar application on soil carbon stocks in the long term and its contribution to the carbon geochemical cycle in the subsoil.

Fine particulate biochar (nano-sized and colloidal biochar) can be transported downward through the soil via macropores.[23−25] This is especially true of aged biochar, the surface of which has more oxygen-containing functional groups as a result of interactions with soil solution, organic and mineral matter, fauna, and microorganisms. The rate of biochar migration through the soil profile is related to application amounts and soil properties.[23,24] The strong mobility of aged biochar in soils indicates that biochar application in topsoil might induce positive or negative feedback of soil carbon in deeper soil depths than that previously estimated. However, according to our current knowledge, no study has investigated the long-term effects of biochar application in topsoil (>10 years) on soil carbon stocks in the subsoil (below 1 m). The impact of biochar application on subsoil carbon dynamics needs to be further understood and quantified to accurately predict and model the long-term effects of biochar on carbon sequestration.

Calcareous soils are prevalent worldwide and make up more than 50% of the world's soils.[14,26,27] Due to biochar's inherent neutral or alkaline properties, the better benefit from biochar-applied field research is gained in acidic croplands, where biochar can improve both soil health and crop yield.[28] One study indicated that lower-temperature straw-derived biochar with nearly neutral pH increased plant growth and OC stocks in calcareous soils.[29] Few studies, however, have examined the subsoil C cycle and C storage of biochar application in calcareous soils. We hypothesize that biochar can move to subsoil after a decade, which has an impact on subsoil inorganic carbon. To address this hypothesis, we investigated the effects of long-term biochar application into topsoil on SOC and SIC stocks in 0−2 m soil depth, especially subsoil (below 1 m).

To explore the mechanisms of C accumulation in these soils, we applied a broad range of isotopic, chemical, microscopic, and spectroscopic techniques to elucidate sources, localization, and chemical composition of C stocks in the soil profile from the topsoil to subsoil. Benzene polycarboxylic acid (BPCA) molecular markers were also tested to prove the presence of biochar in the subsoil. The field-aged biochar was analyzed by Fourier transform infrared spectroscopy (FTIR), X-ray diffraction (XRD), and X-ray photoelectron spectroscopy (XPS). The analyses of scanning electron microscopy (SEM) and scanning transmission electron microscopy with electron energy loss spectroscopy (STEM-EELS) were conducted to investigate the biochar particles found in the subsoil. Our results reveal that the single application of biochar in calcareous cropland after 10 years leads to the significant accrual of SIC in the subsoil, which is much higher than the SOC accumulation. Our study provides conceptual evidence for the key role of fine biochar particle migration on subsoil carbon stocks in calcareous subsoil after a long-term biochar application, which is usually overlooked.

MATERIALS AND METHODS

Location and Experiment Design. The field site is located at the Shangzhuang experimental station of China Agricultural University (Haidian District, Beijing, China, 40° 08′ 21″N, 116° 10′ 52″E, 51 m above sea level). The site has a typical continental monsoon climate, with an annual average air temperature of 11.6 °C and average annual precipitation of 400 mm.[30] The soil is a calcaric Fluvisol, and soil properties are listed in Tables S1 and S2. The crop rotation was winter wheat (*Triticum aestivum* L., from October to June) and summer maize (*Zea mays* L., from June to September). Winter wheat was flood irrigated in early December and mid-May, with a total of 180 mm of water every year, while no irrigation was used for maize. Wheat and maize were fertilized with 112.5, 56.3, and 56.3 kg ha^{-1} N, P, and K, respectively. After harvest, wheat and maize straw was mechanically chopped to 2−3 cm (wheat) and 1−2 cm (maize) pieces, which were rototilled into the 0−0.2 m soil depth for all experiment plots. All the treatments in the experiment returned straw into the field in full amount every year.

Biochar was incorporated into the soil to a depth of 0.2 m in a single application in 2009. The experimental treatments were arranged in a randomized block design with three replicates and included an unamended (control) and three biochar amendment rates (30, 60, and 90 t ha^{-1}). Each plot was 11 m by 10 m in size. Biochar was produced from substrate waste from mushroom production (70% rice husks, and 30% cotton seed hulls) that was pyrolyzed at 400 °C for 4 h. The pyrolysis temperature between 400 and 500 °C, regards as the boundary between low- and high-pyrolysis temperature biochar derived from plant biomass, is the common biochar applied in the field.[12,31,32] Generally, the biochar derived under pyrolysis temperature between 400 and 500 °C can benefit both agricultural and economic fields. The biochar in this study had a particle size of 0.5−5 mm (95% wt) and consisted of 49% organic carbon and 1% inorganic carbon, and the properties of biochar are shown in the Supporting Information (Tables S1−S5).

Soil Sampling and Preparation. Soil samples were taken on April 1st−3rd, 2019. Three soil cores were taken at random locations in each plot from 0 to 2 m depth in 20 cm depth increments by using a 2.5 cm diameter soil auger. The three samples per plot were then composited. The soil cores of control and biochar-amended soils at 0−2 m in 20 cm depth increments were immediately analyzed for water content (wt/wt), pH (1:5 w/v soil to water ratio), and bulk density. A portion of the randomly selected soil samples used for microbial analyses was stored in a −80 °C freezer. After visible plant materials were removed, the remaining portion was air-dried, and passed through a 2 mm stainless steel sieve prior to further analysis.

Properties of Soil and Biochar Particles. Total carbon and nitrogen were analyzed by combustion using an elemental analyzer (Vario EL III, Elementar Analysensysteme GmbH, Germany), and the SOC was also analyzed by the same instrument after removing inorganic carbon using concentrated hydrochloric acid (12 M, 24 h).[33] SIC was calculated as the difference between total and organic carbon. The calcium

https://doi.org/10.1021/acs.est.2c06419
Environ. Sci. Technol. 2023, 57, 1837−1847

carbonate content ($CaCO_3$) was measured based on a method from FAO.[34] Cation exchange capacity was determined through sodium acetate extraction, followed by flame-photometry.[35] For Eh measurement, the soil samples were dried at 35 °C for 3−4 days to obtain more stable measurements, and 25% ultrapure water (Eh about 0.4 V) was added to re-wet the soil samples. Then, multiple measurements (12 times) were conducted using an oxidation−reduction potential meter with frequent cleaning of the electrode.[36] After being measured, according to the Ag/AgCl reference electrode, all potentials versus Ag/AgCl (E) were transformed to give Eh according to the standard hydrogen electrode. The ash content of the biochar was determined as the ratio of residue remaining after combusting the biochar samples at 750 °C for 6 h to the initial mass of biochar after drying at 105 °C.[37] The mineral composition of original and aged biochar particles was scanned in the range of 10−70° using an X-ray diffractometer (XRD, D8 Advance, Bruker, Germany) at a scanning rate of 1° min^{-1}.

Carbon Stocks in SOC, SIC, and Soil Carbonate. The carbon stocks in SOC, SIC, and carbonates at each soil depth were calculated by the following equations

$$C_{SOC} = \sum_{i=1}^{n} C_{SOC,i} \times \rho_{b,i} \times D_i \quad (1)$$

$$C_{SIC} = \sum_{i=1}^{n} C_{SIC,i} \times \rho_{b,i} \times D_i \quad (2)$$

$$C_{CaCO_3} = \sum_{i=1}^{n} C_{CaCO_3} \times \rho_{b,i} \times D_i \times \left(1 - \frac{F_i}{100}\right) \quad (3)$$

where C_{SOC}, C_{SIC}, and C_{CaCO_3} are the carbon stocks in SOC, SIC, and carbon of carbonates (t ha^{-1}) at 0−2 m depth, respectively. The subscript i represents the i-th depth increment (0−0.2, 0.2−0.4,..., 1.8−2.0 m) with n = 10. $C_{SOC,i}$, $C_{SIC,i}$, $C_{CaCO_3,i}$, $\rho_{b,i}$, and F_i are the carbon contents (g kg^{-1}) of SOC, SIC, carbonate, soil bulk density (kg m^{-3}), and the volumetric percentage of the fractions >2 mm (rock fragments) at depth i, respectively. D_i is the length of the depth increment i (cm).

$\delta^{13}C$ Determination. The $\delta^{13}C$ of SOC ($\delta^{13}C_{SOC}$) for unamended control and biochar-amended soils over the 0−2 m soil depth were measured using an isotope ratio mass spectrometer (IsoPrime IRMS, GV Instruments, Manchester, U.K.). The $\delta^{13}C$ of biochar-organic carbon (biochar-OC) for the original (2009) and the field-aged biochar (obtained in 2019) were also measured. The $\delta^{13}C_{SOC}$ values of the surface soil (0−0.2 m depth) were −24.26 ± 0.40‰ (control), −24.33 ± 0.24‰ (30 t ha^{-1}), −25.46 ± 0.08‰ (60 t ha^{-1}), and −25.59 ± 0.20‰ (90 t ha^{-1}), respectively. There was no difference in the $\delta^{13}C_{OC}$ between the original (−26.50 ± 0.08‰) and aged (−26.50 ± 0.01‰) biochar, which indicated that the aging process had no effect on the $\delta^{13}C$ of the biochar-OC.

The control and biochar-amended soil samples of 5.000 mg were accurately weighed in a Labco reaction flask (12 mL- with a headspace cap), and the sample was purged with He gas for 5 min to remove the air in the flask. After the aeration is complete, the pressure inside the bottle was adjusted to the atmospheric pressure. A syringe needle was inserted into the sample bottle to drain excess helium. When venting, one end of the needle was inserted into the sample bottle and the other end of the tube was completely submerged in water. During this process, air should be avoided entering the sample bottle. Then, 0.1 mL of phosphoric acid was extracted and poured into the bottle from the edge of the gasket on the bottle cap. The phosphoric acid was directly dropped into the bottom of the bottle. The bottle was shaken to make the acid fully mixed with the sample. The CO_2 of inorganic carbon from biochar-inorganic carbon (biochar-IC), the unamended control soil, and biochar-amended soils were collected from an enclosed system where biochar/soil samples were fully reacted with 100% H_3PO_4 for 3 h at 70 °C. The collected CO_2 was then analyzed for isotopic analysis using an isotope ratio mass spectrometer MAT-253 (Thermo Fisher Scientific, Inc., Bremen, Germany). The $\delta^{13}C$ of both SIC and biochar-IC were expressed relative to the international standard of Pee Dee Belemnite (PDB). The $\delta^{13}C$ of biochar-IC after 10 years also did not change (−11.28 ± 0.09‰ for original biochar and −11.24 ± 0.10‰ for aged biochar).

Spectroscopic Analysis. The microstructure and elemental composition of the unamended control and biochar-amended soils (60 and 90 t ha^{-1} biochar application rates) at the 0−0.2 m (biochar-applied soil depth) and 1.4−1.6 m (biochar-migration soil depth) were investigated using scanning electron microscopy (SEM, Nova Nano SEM450, FEI, U.S.A.) coupled with energy-dispersive X-ray analysis (EDS, EDAX, Octane SDD, Apollo XLT SDD, U.S.A., and a Phenom Pro-X FEI, Netherlands). The biochar-amended soil at the 1.8−2.0 m soil depth was investigated by STEM with EDS and EELS analysis. STEM analysis was conducted using a JEOL ARM 200F instrument operating at 200 kV (JEOL, Japan), equipped with high angle annular dark-field (HAADF) and bright-field (BF) detectors. EDS analysis was performed using a JEOL EDS detector coupled to a Noran System Seven analytical system (Thermo Scientific, U.S.A.), and EELS analysis was conducted with a GIF Quantum energy filter. The system had an energy resolution of 0.5 eV.

BPCA Determination. The concentration of BPCAs in biochar and soil samples was measured following methods described in Brodowski et al.[38] Briefly, trifluoroacetic acid (TFA, 10 mL, 4 M) was used to digest biochar/soil samples (containing 5 mg organic carbon) at 105 °C for 4 h. After the residue was cooled, it was washed several times with deionized water, filtered through a Whatman glass fiber filter (GF/a 1.6 μm), and dried at 40 °C for 3 h. After the residue was transferred into a Teflon-lined bomb, nitric acid (2 mL, 65%) was added to the bomb and stored in a high-pressure digester for reaction at 170 °C for 8 h. The mixture was then filtered through an ashless cellulose filter and purified. The digested solution (2 mL) was diluted with deionized water (10 mL), and an internal standard was selected with citric acid (100 μL). A cation exchange resin (Dowex 50 WX8, 200−400 mesh) was used to treat the solution. After freeze-drying, the treated aqueous sample was re-dissolved in methanol. The sample was dried with N_2 and derivatized into trimethylsilyl derivatives for gas chromatography-mass spectrometer analysis using 7890A GC equipped with a 5975C quadrupole mass selective detector (Agilent, U.S.A.). All samples were analyzed with four replicates.

Statistical Analyses. Statistical differences between the unamended control and biochar-amended soils were analyzed by one-way analysis of variance (ANOVA, IBM SPSS Statistics 22.0) to assess the effects of biochar application on soil carbon (SOC, SIC, and carbonate). Statistical differences in the

https://doi.org/10.1021/acs.est.2c06419
Environ. Sci. Technol. 2023, 57, 1837−1847

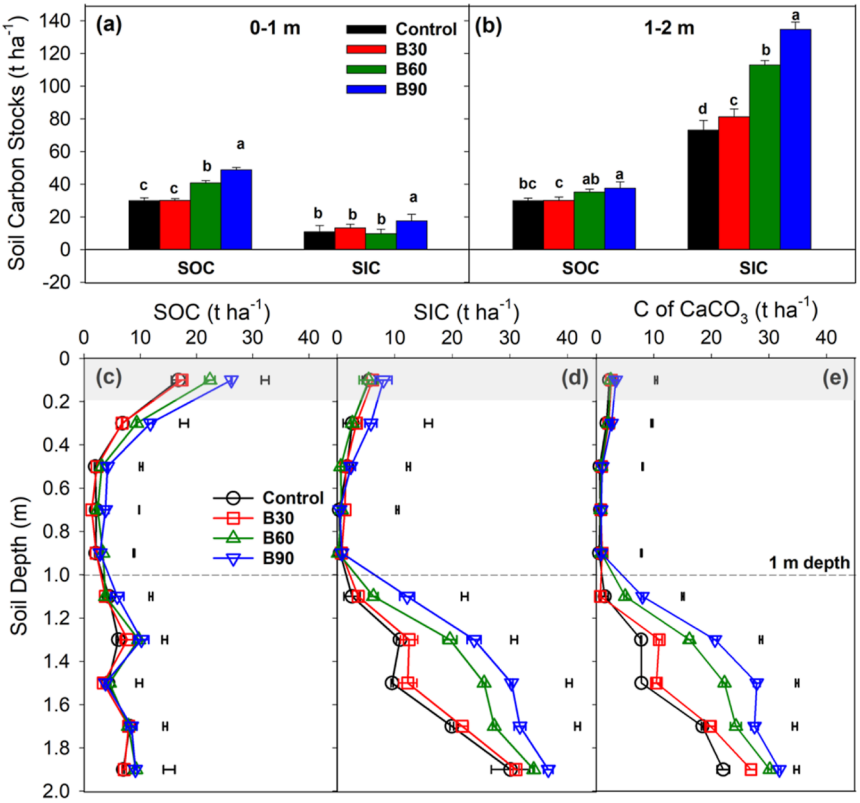

Figure 1. Effects of biochar on soil organic and inorganic carbon stocks through the soil profile 10 years after a single biochar application to top 20 cm soil. SOC and SIC stocks at (a) 0−1 and (b) 1−2 m in the control and biochar-amended soils after 10 years. The distributions of (c) SOC, (d) SIC, and (e) carbon present as calcium carbonate in soil profile (0−2 m) in increments of 0.2 m. The lowercase letters indicate significant differences in (a,b). The error bars in c to e are the least significant differences (LSDs) at a confidence level of 5%. Control, B30, B60, and B90 represent the biochar application rates of 0, 30, 60, and 90 t ha^{-1}, respectively.

distribution of carbon (including SOC, SIC, the carbon of soil carbonate), the $\delta^{13}C$ of SOC and SIC in the soil profile between the unamended control and biochar-amended soils were tested through least significant difference (Fisher's LSD) at the confidence level of 5%. The statistical significance of the regression function was analyzed using an unpaired two-sided *t*-test.

RESULTS AND DISCUSSION

Biochar-Driven Acculturation of SIC in the Subsoil. Biochar amendments increased SIC, particularly in the subsoil (Figure 1a,b). Compared to the unamended control, SIC was increased by 11.2% (B30), 54.5% (B60), and 84.3% (B90) at the soil depth of 1−2 m (Figure 1b). Biochar amendment mainly increased the SOC in the depths at 0−1 m in reference to the control soil (Figure 1a,c). The SIC showed a significant increase at subsoil (especially soil depth 1.2−1.6 m) (Figure 1d). Calcium carbonate also largely grew correspondingly in the subsoil (Figure 1e), and magnesium carbonate occupied no more than 21.2% of SIC in the subsoil (Figure S1), which suggested that calcium carbonate was the main component of SIC in this soil. At 0−2 m, SOC increased by 0.4% (B30), 26.7% (B60), and 44.3% (B90). Within the 0−2 m profile, the SIC increases in B60 and B90 were 2.4 to 2.6 times higher than the SOC increase. The total soil carbon (i.e., existing SOC, SIC, and biochar-C) increased by 71, 182, and 210% for B30, B60, and B90, respectively.

Effect of Biochar Application on the $\delta^{13}C$ from Topsoil to Subsoil. Biochar application also influenced the ^{13}C signatures of SOC ($\delta^{13}C_{SOC}$) and SIC ($\delta^{13}C_{SIC}$) (Figure 2a,b). Briefly, biochar amendments caused the more negative $\delta^{13}C$ (OC and IC) in the topsoil due to the inherent ^{13}C signature of the biochar (Materials and Methods section). For the $\delta^{13}C_{SOC}$, it was obvious that the soil amended by biochar had a more negative $\delta^{13}C_{SOC}$ for 0−2 m depth, which could be attributed to the more negative ^{13}C signature of biochar ($\delta^{13}C_{OC}$ = −26.50 ± 0.08‰, in the Materials and Methods section). Because the biochar-OC accounted for 98% of biochar-C, biochar migration was responsible for the change of $\delta^{13}C_{SOC}$. This was strong evidence that biochar particles were transported with water movement from topsoil to subsoil after 10 years.

Although the biochar-IC just accounted for 1% of biochar, it also affected the $\delta^{13}C_{SIC}$, especially in the topsoil, where biochar was plentiful. It was interesting that the $\delta^{13}C_{SIC}$ above and below 1 m showed different change trends. The $\delta^{13}C_{SIC}$ above 1 m was more negative than below 1 m (Figure 2b), which suggested that the SIC in the surface soil and subsoil had different carbon sources. For 0−20 cm, the $\delta^{13}C_{SIC}$ of biochar-amended soils had more negative signatures than the control soil due to the more negative isotopic signature of the biochar-IC (−11.28 ± 0.09‰). At soil depths from 0.2 to 1 m, the vertically migrated biochar did not significantly change the signature of $^{13}C_{SIC}$. The reason might be that the biochar contained only 1% IC (0.3, 0.6, and 0.9 t ha^{-1} for B30, B60, and B90, respectively); thus, the migration of biochar with low biochar-IC was difficult to affect the $\delta^{13}C_{SIC}$ of soil significantly. This also demonstrated that the increased IC

https://doi.org/10.1021/acs.est.2c06419
Environ. Sci. Technol. 2023, 57, 1837−1847

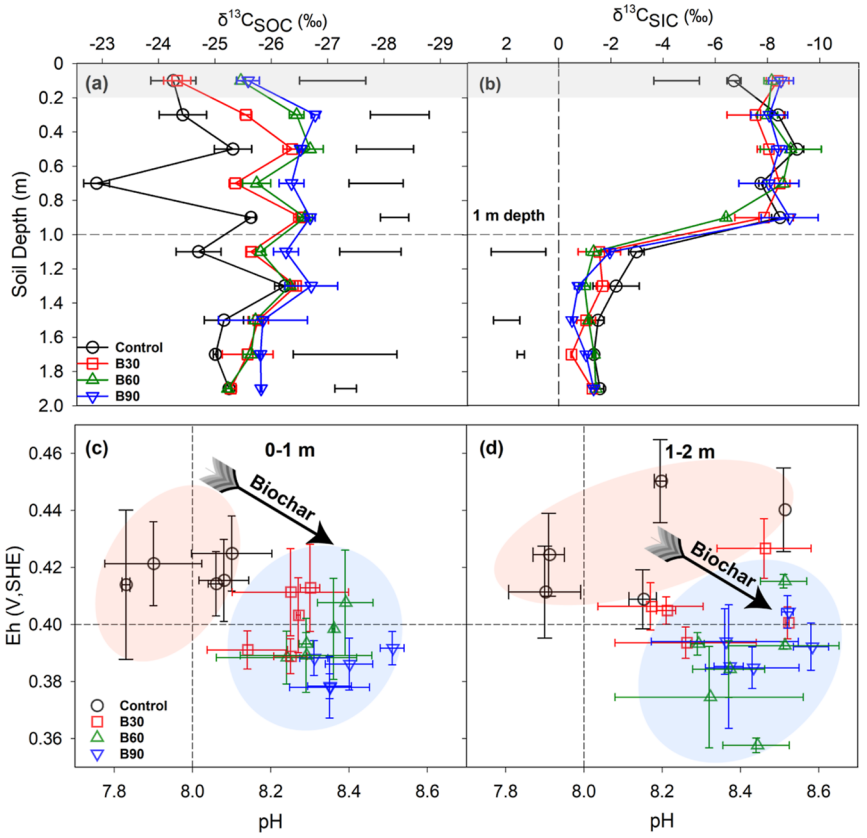

Figure 2. Effects of biochar on ^{13}C signatures and Eh-pH diagrams 10 years after a single biochar application to topsoil. The distribution of (a) SOC ^{13}C signature ($\delta^{13}C_{SOC}$), (b) SIC ^{13}C signature ($\delta^{13}C_{SIC}$), and (c) soil pH as a function of soil depth. The Eh-pH diagrams at depth (d) 0−1 and (e) 1−2 m. The areas of light-red and light-blue denoted the control and biochar-amended soils, respectively. The arrows in (d,e) show the direction of the biochar effect. The error bars in a to c are the LSD at a confidence level of 5%. Control, B30, B60, and B90 represent the biochar application rates of 0, 30, 60, and 90 t ha^{-1}, respectively.

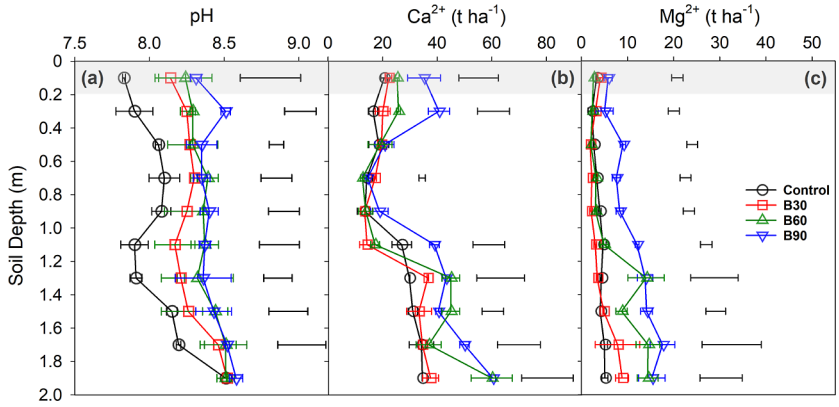

Figure 3. Effects of biochar on (a) soil pH and the retention of (b) Ca and (c) Mg in subsoil 10 years after a single biochar application to topsoil. The significant differences of (b) Ca^{2+} and (c) Mg^{2+} between unamended control and biochar-amended soils were evaluated using the LSD method at a confidence level of 5%. Control, B30, B60, and B90 represent the biochar application rates of 0, 30, 60, and 90 t ha^{-1}, respectively.

stocks of biochar-amended soils were not from the IC of biochar. Interestingly, for subsoils, biochar amendment resulted in less negative isotope signature, which further indicated that biochar amendment changed the composition of SIC in the subsoil. Biochar amendment can improve the soil structure[39−41] and may influence the interaction between shallow groundwater and the subsoil to some extent.

Effect of Biochar Application on soil pH, Ca, and Mg. Furthermore, the soil pH value was higher in the biochar-amended soils than that in the control soil (Figure 2c,d). Even in the subsoil (1 m-1.8 m), the pH also increased from 7.8 to 8.0 (control soil) to 8.2−8.6 (biochar-amended soils). The inherent alkalinity (pH 9.8 ± 0.2) and high ash content (36.3%) of biochar contributed to the increase in soil pH (Table S1). Interestingly, biochar amendment also decreased the soil pH and Eh simultaneously, further changing the subsoil (micro) environmental conditions, which were consistent with previous studies.[12,42] In the subsoil, except for the alkalinity from biochar, the HCO_3^- uprising from shallow groundwater increased the alkalinity of biochar-

https://doi.org/10.1021/acs.est.2c06419
Environ. Sci. Technol. 2023, 57, 1837−1847

amended soils because biochar caused better root growth[43] and greater evapotranspiration, and carbonates were easier to precipitate and recrystallize in the biochar-amended subsoil. The pH can affect carbonate crystal size and morphology by controlling the supersaturation state of soil solution with $CaCO_3$.[44] The ratio of bicarbonate/carbonate can decrease as the soil pH becomes alkaline, which can cause higher nucleation rates and faster precipitation of $CaCO_3$ crystals with smaller size.[44,45] If there are sufficient CO_2, CO_3^{2-}, and HCO_3^- in the soil environment, available Ca and Mg carbonates can be easily precipitated or formed in this pH range. Typically, CO_2 concentrations in subsoils are consistently high, up to 100 times greater than the atmospheric CO_2 concentration.[46] The increased pH of the biochar amendments along with the high CO_2 concentration might result in an energetically favorable environment for the precipitation of $CaCO_3$ and $MgCO_3$.[47−49]

An adequate supply of Ca^{2+} and Mg^{2+} is another prerequisite for the formation of carbonates. The high contents of Ca^{2+} and Mg^{2+} cations were observed in the biochar-amended soils (Figure 3b,c). Biochar amendment (90 t ha^{-1}) largely increased the stocks of Ca in 0−0.4 m and Mg below 0.4 m. The mineral fertilizer applied in topsoil twice every year induced carbonate dissolution.[26,50,51] Compared to the control, biochar amendments with 60 and 90 t ha^{-1} increased the contents of soil Ca and Mg below 1.2 m ($p < 0.05$). Above 1 m, there was a negative relationship between Ca^{2+} and Mg^{2+} for all the biochar amendments except B30 (Figure S2a). Interestingly, below 1 m, the Mg^{2+} showed a positive linear relationship with the Ca^{2+} in both control and biochar-amended soils (Figure S2b). This was the strong evidence that a large amount of Ca^{2+} and Mg^{2+} came from shallow groundwater fluctuation (periodic rising or falling). The Ca^{2+} and Mg^{2+} can rise together with shallow groundwater when strong evapotranspiration occurs (e.g., at summer). As irrigation or precipitation happens, both Ca^{2+} and Mg^{2+} are leached down. Because the solubility of Mg^{2+} is much higher than the solubility of Ca^{2+},[52,53] Mg^{2+} is leached deeper and quicker than Ca^{2+}. Therefore, in the 0−1 m, the correlation between Ca^{2+} and Mg^{2+} was negative because more Mg^{2+} and less Ca^{2+} were leached down (except B30), but below 1 m, the correlations were positive because both Ca^{2+} and Mg^{2+} upraised under strong evapotranspiration conditions. Because the biochar-amended subsoil had sufficient Ca^{2+} and CO_2 along with Mg^{2+}, it might be both energetically and kinetically favorable for producing the precipitation of $CaCO_3$, $MgCO_3$, or $Mg(HCO_3)_2$.[27,48,49]

Direct Evidence of Biochar Migration into Subsoil. Biochar amendments increased the BPCA content from the topsoil to the subsoil (Figure 4 and Table S4). BPCA is a widely used marker for qualitative and quantitative black carbon (including biochar) in the soil. BPCA is the sum of B3CAs (sum of trimellitic acid, hemimellitic acid, and trimesic acid), B4CAs (sum of mellophanic acid, prehnitic acid, and pyromellitic acid), B5CA (benzenepentacarboxylic acid), and B6CA (mellitic acid).[38] The BPCA content in 1.4−1.6 m depth of 60 t ha^{-1} biochar-amended soil was 6.8 times higher than that in the control soil (Table S4), which directly demonstrated that biochar moved downward from the topsoil to the subsoil over the 10-years period. In addition, compared with the control, the soil suspensions of B60 after 24 h of settling showed a darker color in the entire soil profile from the topsoil to the subsoil, indicating that the fine biochar particles might be transported to the subsoil and lead to the darker color of the biochar-amended soil suspension (Figure S3). The other biochar-amended soils (B30, B90) were also darker than the control from the topsoil to the subsoil.

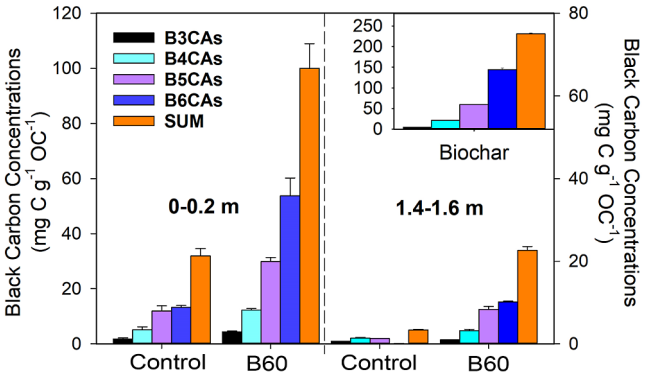

Figure 4. Black carbon contents in (a) topsoil (0−0.2 m) and (2) selected subsoil (1.4−1.6 m) 10 years after a single biochar application. The black carbon contents were analyzed by BPCA method for biochar, the control, and biochar-amended soil (60 t ha^{-1}, B60) in the topsoil and selected subsoil. BPCA individual chemicals were summarized (SUM) into different groups containing B3CAs (sum of trimellitic acid, hemimellitic acid, and trimesic acid), B4CAs (sum of mellophanic acid, prehnitic acid, and pyromellitic acid), B5CA (benzenepentacarboxylic acid), and B6CA (mellitic acid).

Fine biochar particles are mobile and can move vertically along with irrigation and rainfall.[23,54] In particular, aged biochar particles had stronger mobility than pristine biochar because aging process decreases biochar size, and increases the oxygen-containing functional groups and the hydrophilicity on its surface.[24] The spectral and energy spectrum were used to characterize the changes in surface properties of biochar during aging processes (Figure S3). The FTIR analysis showed that the peaks of oxygen-containing functional groups, that is, hydroxyl (3380 cm^{-1}), quinones (1750 cm^{-1}), carboxyl (1500−1650 cm^{-1}), and phenol (1030 cm^{-1}) increased in the 10-years field-aged biochar selected from topsoil compared with the original biochar (Figure S4a). Our results were consistent with the finding from Weng et al. (2017), which compared the original biochar with the 9.5-years field-aged biochar.[9] The XRD results from the original and field-aged biochar presented that in addition to obvious graphite/quartz crystals on the surface of biochar, $CaCO_3$ was precipitated onto the surface of field-aged biochar (Figure S4b). Similarly, according to XPS, both $CaCO_3$ and oxygen-containing functional groups were increased on the surface of the field-aged biochar (Table S5). In addition, after 10 years of field aging, the surface of aged biochar showed cracking, suggesting the pristine biochar was broken up into smaller biochar particles (Figure S5), which created reactive surfaces that could facilitate redox and acid-base reactions as well as adsorption of both inorganic ions and organic molecules.[55] The migrated rates of biochar showed the positive correlationship with the amount of applied biochar in topsoil due to the change of the topsoil physi-chemical properties.[23] Thus, B60 and B90 treatments might cause higher black carbon concentration in the subsoil, which could induce more SIC precipitation in the B60 and B90 subsoil.

Carbonate Precipitation on Biochar Particles in Subsoil. Biochar particles extracted from subsoil were investigated by a series of spectral and energy spectral analyses.

https://doi.org/10.1021/acs.est.2c06419
Environ. Sci. Technol. 2023, 57, 1837−1847

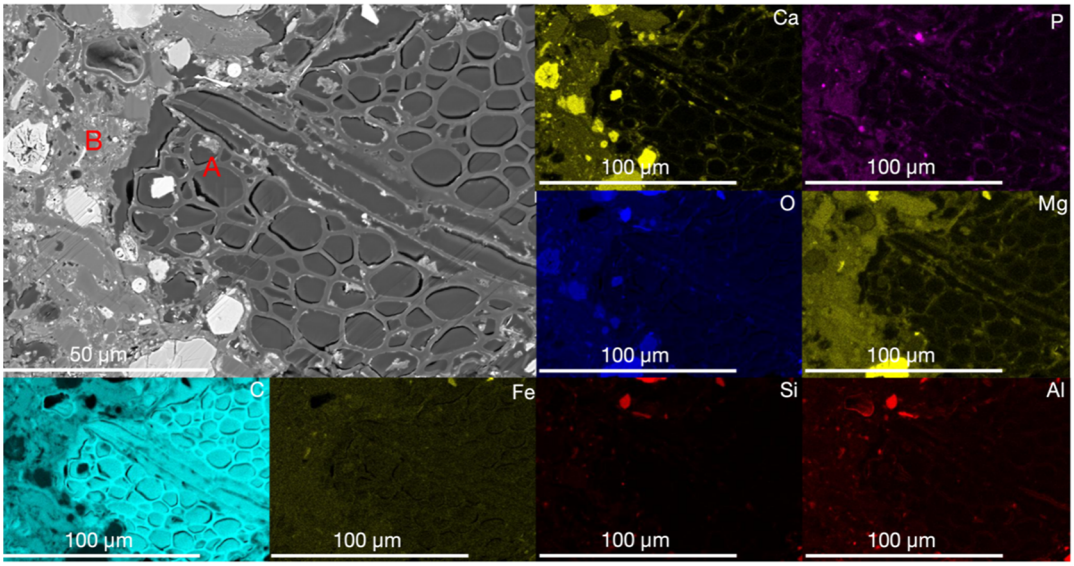

Figure 5. Spectroscopic analysis of biochar particles in subsoil at the biochar-amended plots 10 years after a single biochar application. Identification of $CaCO_3$ precipitation on biochar surface and pores in the biochar-amended subsoil. Backscattered electron image of a focused ion beam (FIB) section containing resin-impregnated biochar (area A) and soil (area B), and the EDS maps of the distribution of the main elements C, Ca, O, Mg, Al, Si, P, and Fe. The biochar-soil particles were extracted at the depth of 1.4−1.6 m in biochar-amended soil 10 years after a single biochar application.

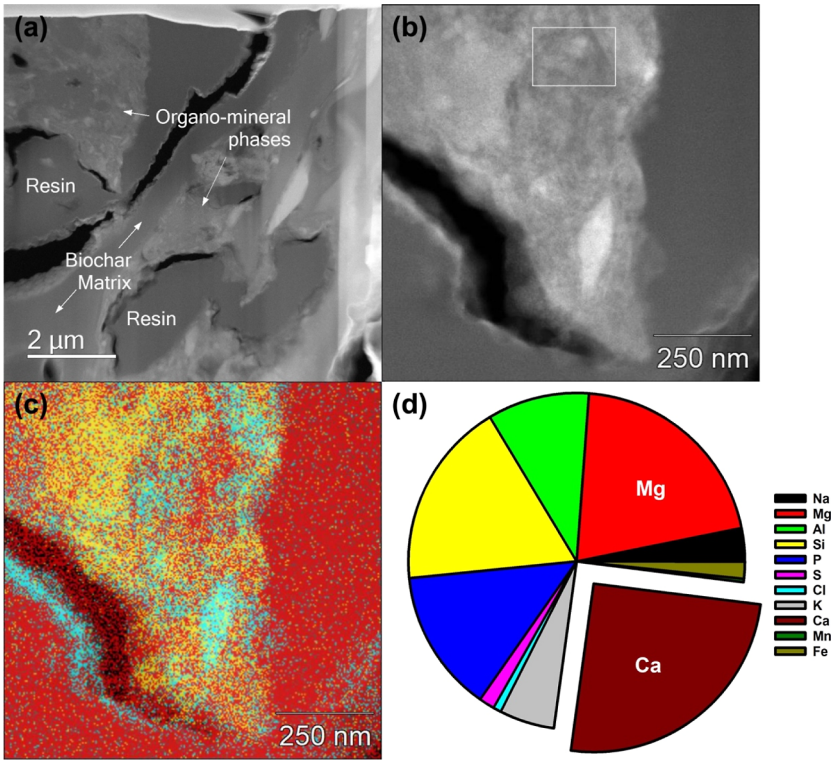

Figure 6. Analysis of organo-mineral components of the biochar and the mineral layers 10 years after a single biochar application. (a) HAADF images of biochar carbon pores and the organo-mineral phase inside the pores; (b) detail of (a) showing the organo-mineral phase; (c) phase map of (b), red-predominantly carbon in the biochar, yellow-apatite, and cyan-Ca/Mg silicate; (d) an analysis of the boxed region in (b) showing that the main elements (atomic %, excluding C and O) are Ca, Mg, P, K, and Si.

Electron microscopy, energy-dispersive spectroscopy (EDS) spectra, and energy electron loss spectroscopy (EELS) of both the external surfaces and internal pores of the biochar extracted from a soil depth of 1.4−1.6 m revealed that nanoparticulate $CaCO_3$, $MgCO_3$, and dolomite, as well as compounds rich in Al, Si, P, K, Na, Cl, and Fe were formed inside and on the external surface of the biochar particles (Figures 5 and S6). $Ca_3(PO_4)_2$, clay with K and Fe in the lattice, SiO_2, iron oxides, and chlorides were also detected. These were bound together by organic compounds. The nanoparticulate $CaCO_3$ crystal cluster was identified in approximately 20 μm from a large biochar particle (Figures 5, S6, and S7). The EDS and EELS

https://doi.org/10.1021/acs.est.2c06419
Environ. Sci. Technol. 2023, 57, 1837−1847

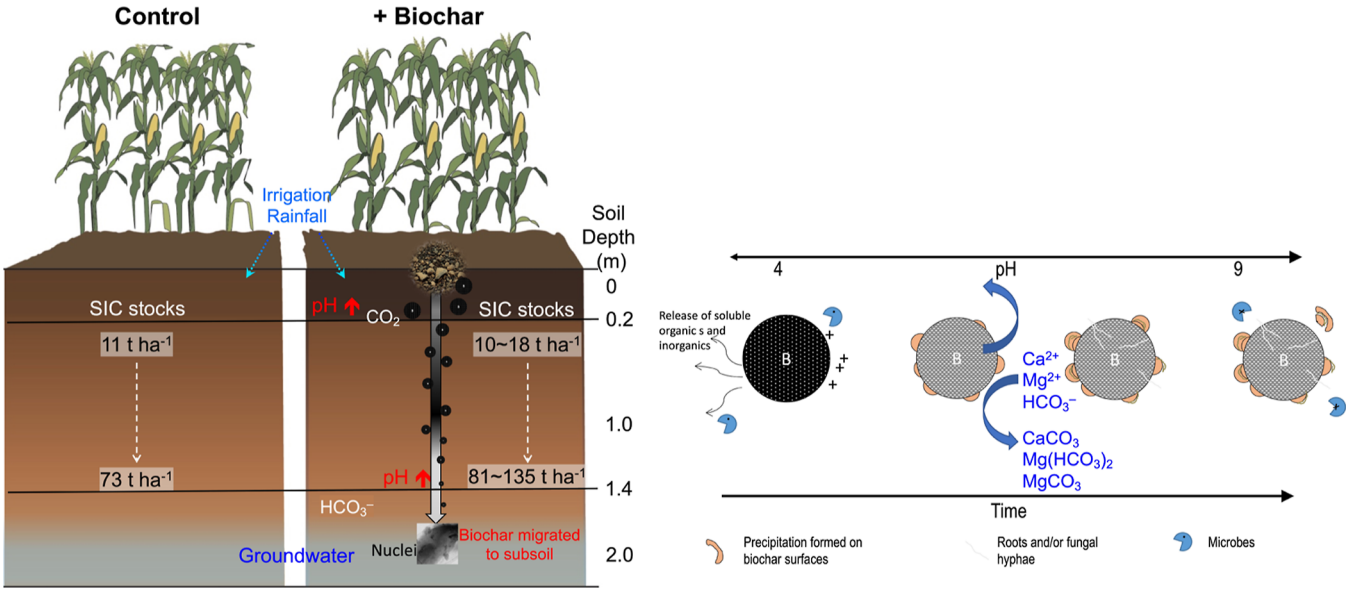

Figure 7. Proposed mechanisms of SIC accrual in calcareous subsoil 10 years after a single biochar application to top 20 cm soil. In 0−1 m depth, SIC was slightly increased by biochar. In the 1−2 m depth, there was substantial SIC accrual (93−95% increase) because of the followings: (1) biochar particles moved to subsoil, subsoil pH increased to 8.2−8.6, and the pH increase resulted in more carbonate precipitation after saturation; (2) the external and internal (pore) surfaces of biochar provided nuclei for the precipitation of Ca and Mg carbonates in subsoil.

spectra indicated that this cluster had formed on small biochar particle that might be fractured from the main particle. The HAADF image in Figure S7a shows the mixed (Ca/Mg)CO_3 nanoparticles (bright region) adjacent to a micron-sized biochar particle coated with mineral-rich (Ca and Mg) organic compounds. The interesting and inspiring part is that the EELS 4 spectrum of Figure S6a from the carbonate shows a very different edge structure to the amorphous carbon of the biochar (EELS 1) and organo-mineral layer (EELS 2−3). Figure S7c clearly shows the HAADF detail of (a), which exhibits the organo-mineral layer between the biochar (bottom) and the carbonate phase (top). These spectral images provided an exciting result for our study. Inorganic minerals such as $CaCO_3$, $MgCO_3$, and dolomite were found on the surface of biochar particles that migrated into the subsoil. All the evidence supported that biochar particles can act as nuclei to precipitate SIC in the subsoil. Similarly, the greater contents of $CaCO_3$, $KHCO_3$, $CaMgSiO_2$, and probably SiO_2 were found on internal and external surfaces of the 10-year aged biochar extracted from the topsoil (Figure S4b). These results provided direct evidence that long-term biochar application was not only beneficial to soil carbon sequestration in the topsoil but also largely increased SIC in subsoil due to the migration of biochar particles into the subsoil.

Mechanism. This study provides strong evidence that biochar with high application rate can increase the accumulation of SIC in subsoil (Figure 1). The analysis of the soil properties and the biochar at the macro-, micro-, and nano-scale was conducted to prove the possible mechanisms. A single addition of biochar into calcareous topsoil (especially at higher application rates) significantly increased the soil pH from topsoil to subsoil after a decade. Biochar had migrated through the soil to a depth of 2 meters after 10 years, and the organo-mineral phases formed in the pores of the biochar and on its external surfaces. The biochar particles in subsoil provided the nuclei for SIC precipitation (Figures 5 and 6). Two mechanisms (Figure 7) are proposed to explain how biochar induces SIC accrual in the subsoil. (i) Biochar particles migrate to the subsoil and elevate the soil pH by 0.2−0.5 units, which causes favorable pH conditions for the precipitation of Ca and Mg carbonates.[47] (ii) The external and internal (pore) surfaces of aged biochar provide nuclei for the precipitation of Ca and Mg carbonates.[56−59] These carbonates are incorporated into the organo-mineral phase on the external and internal surfaces of the biochar pores. As biochar ages in soil, it fractures, and new surfaces are formed allowing further carbonate precipitation.

In this study, after the addition of biochar which contributed to 15, 30, and 45 t C ha^{-1} SOC, the SIC in biochar-amended soils increased by 10, 38, and 68 t ha^{-1} after 10 years, respectively. In the long-term, biochar application on calcareous soil can directly sequester OC and especially indirectly precipitate IC through increasing soil pH and providing reactive nuclei, which can induce accrual SIC in subsoil below 1 m. For the first time, we have shown the biochar-enhanced SIC accumulation in the subsoil. It is important to stress that this substantial increase in SIC resulted from a large one-time investment in biochar amendment. It should be emphasized that long-term biochar field application affects soil C not only in topsoil but also in subsoil. Especially, the effect on SIC in subsoil (below 1 m) is always neglected in current research. The insights from this study will advance the current understanding for the impact of biochar application on C dynamics in the subsoil, which is beneficial to soil carbon storage, soil health, and productivity. Our dramatic findings need to be confirmed through more trials on other filed sites. Therefore, it is necessary to conduct more long-term biochar field experiments to better clarify the impact of long-term biochar application on subsoil C sequestration in the field.

Environmental Implications. Our study showed that SIC stocks in the subsoil at a depth of 1−2 m increased by 11−84% over 1 decade after single biochar additions into calcareous topsoil. The reason might be that the biochar particles after 10 years migrated into subsoil, and this caused the increase in

https://doi.org/10.1021/acs.est.2c06419
Environ. Sci. Technol. 2023, 57, 1837−1847

subsoil pH and the migrated biochar became reactive nuclei for HCO_3^- and CO_2 precipitation in subsoil. Sequestration of inorganic carbon through biochar amendments to calcareous topsoil was of a similar magnitude after 1 decade as organic carbon sequestration in biochar itself. This study provided vital evidence for the impact of biochar application on carbon stocks in the subsoil in the long run.

The impact of biochar on SIC in subsoil must be understood to inform strategies for atmospheric carbon dioxide removal through biochar application to calcareous soils in the long term. Insights from this study advance our current understanding of soil carbon dynamics, especially the significance of SIC storage and persistence in calcareous soils. Our study provides proof for the concept that biochar application to topsoil induces SIC changes in the subsoil and associated geochemical impact. Understanding the role of biochar on subsoil carbon dynamics is critical for international terrestrial carbon sequestration and climate prediction in the coming decades to centuries. Further studies are needed to understand the effects of biochar on SIC dynamics and the mitigation potential of biochar in various types of soil.

■ ASSOCIATED CONTENT

Supporting Information

The Supporting Information is available free of charge at https://pubs.acs.org/doi/10.1021/acs.est.2c06419.

The supporting information includes additional figures and tables as referenced in the manuscript text (PDF)

■ AUTHOR INFORMATION

Corresponding Author

Jianying Shang − *College of Land Science and Technology, Key Laboratory of Arable Land Conservation (North China), Ministry of Agriculture, China Agricultural University, Beijing 100193, China;* orcid.org/0000-0002-2498-9699; Email: jyshang@cau.edu.cn

Authors

Yang Wang − *College of Land Science and Technology, Key Laboratory of Arable Land Conservation (North China), Ministry of Agriculture, China Agricultural University, Beijing 100193, China;* orcid.org/0000-0002-6855-7097

Stephen Joseph − *School of Materials Science and Engineering, University of New South Wales (NSW), Sydney 2052 New South Wales, Australia*

Xiang Wang − *College of Land Science and Technology, Key Laboratory of Arable Land Conservation (North China), Ministry of Agriculture, China Agricultural University, Beijing 100193, China*

Zhe H. Weng − *School of Agriculture and Food Sciences, The University of Queensland, St. Lucia 4072 Queensland, Australia;* orcid.org/0000-0002-9567-095X

David R.G. Mitchell − *Electron Microscopy Centre, Innovation Campus, University of Wollongong, North Wollongong 2517 New South Wales, Australia*

Mitchell Nancarrow − *Electron Microscopy Centre, Innovation Campus, University of Wollongong, North Wollongong 2517 New South Wales, Australia*

Sarasadat Taherymoosavi − *School of Materials Science and Engineering, University of New South Wales (NSW), Sydney 2052 New South Wales, Australia*

Paul Munroe − *School of Materials Science and Engineering, University of New South Wales (NSW), Sydney 2052 New South Wales, Australia*

Guitong Li − *College of Land Science and Technology, Key Laboratory of Arable Land Conservation (North China), Ministry of Agriculture, China Agricultural University, Beijing 100193, China*

Qimei Lin − *College of Land Science and Technology, Key Laboratory of Arable Land Conservation (North China), Ministry of Agriculture, China Agricultural University, Beijing 100193, China*

Qing Chen − *College of Resources and Environmental Science, Beijing Key Laboratory of Farmland Soil Pollution Prevention and Remediation, China Agricultural University, Beijing 100193, China*

Markus Flury − *Department of Crop and Soil Sciences, Washington State University, Puyallup, Washington 98374, United States; Department of Crop and Soil Sciences, Washington State University, Pullman, Washington 99164, United States;* orcid.org/0000-0002-3344-3962

Annette Cowie − *School of Environmental and Rural Science, University of New England, Armidale 2351 New South Wales, Australia; NSW Department of Primary Industries, Armidale 2351 New South Wales, Australia*

Olivier Husson − *Centre de Coopération Internationale en Recherche Agronomique pour le Développement (CIRAD), Montpellier F-34398, France; Unité Propre de Recherche Agroécologie et Intensification Durable des Cultures Annuelles (UPR AIDA), Montpellier F-34398, France; AIDA, Université de Montpellier, CIRAD, Montpellier F-34398, France*

Lukas Van Zwieten − *NSW Department of Primary Industries, Wollongbar Primary Industries Institute, Wollongbar 2477 New South Wales, Australia*

Yakov Kuzyakov − *Department of Soil Science of Temperate Ecosystems, Department of Agricultural Soil Science, University of Göttingen, Göttingen 37077, Germany; Peoples Friendship University of Russia (RUDN University), Moscow 117198, Russia*

Johannes Lehmann − *Soil and Crop Science, School of Integrative Plant Science, Cornell University, Ithaca, New York 14853, United States;* orcid.org/0000-0002-4701-2936

Baoguo Li − *College of Land Science and Technology, Key Laboratory of Arable Land Conservation (North China), Ministry of Agriculture, China Agricultural University, Beijing 100193, China*

Complete contact information is available at: https://pubs.acs.org/10.1021/acs.est.2c06419

Author Contributions

Conceptualization: Y.W., J.Y.S., G.T.L., and Q.M.L.; methodology: S.J., Y.W., J.Y.S., J.L., X.W., and O.H.; investigation: Y.W. and J.Y.S.; visualization: Y.W., S.J., W.Z.H., Y.K., X.W., Y.L., D.M., M.N., and S.T.; supervision: J.Y.S.; writing—original draft: Y.W., J.Y.S., and S.J.; and writing—review and editing: Y.W., S.J., A.C., Y.K., W.Z.H., X.W., M.F., L.Z., P.M., Q.C., and B.G.L.

Notes

The authors declare no competing financial interest.

Data and materials availability: all data are available in the main text or the Supporting Information.

https://doi.org/10.1021/acs.est.2c06419
Environ. Sci. Technol. 2023, 57, 1837−1847

■ ACKNOWLEDGMENTS

We thank Prof. Bo Pan (Kunming University of Science and Technology, China) for providing the BPCA determination. This work was supported by National Natural Science Foundation of China (41771255 and 42177278), China Agriculture Research System of Ministry of Finance (MOF) and Ministry of Agriculture and Rural Affairs (MARA) (CARS-23-B15), and The RUDN University Strategic Academic Leadership Program.

■ REFERENCES

(1) Allen, M.; Babiker, M.; Chen, Y.; Zickfeld, K.Summary for Policymakers. In: Global warming of 1.5 °C. *Intergovernmental Panel on Climate Change (IPCC) Special Report*, 2018.

(2) Arneth, A.; Barbosa, H.; Benton, T. G.; Calvin, K.; Pereira, J. P.Summary for Policymakers. In: Climate Change and Land: an IPCC special report on climate change, desertification, land degradation, sustainable land management, food security, and greenhouse gas fluxes in terrestrial ecosystems. *Intergovernmental Panel on Climate Change (IPCC) Special Report*, 2019; pp 1−98.

(3) Cavicchioli, R.; Ripple, W. J.; Timmis, K. N.; Azam, F.; Bakken, L. R.; Baylis, M.; Behrenfeld, M. J.; Boetius, A.; Boyd, P. W.; Classen, A. T.; Crowther, T. W.; Danovaro, R.; Foreman, C. M.; Huisman, J.; Hutchins, D. A.; Jansson, J. K.; Karl, D. M.; Koskella, B.; Mark Welch, D. B. M.; Martiny, J. B. H.; Moran, M. A.; Orphan, V. J.; Reay, D. S.; Remais, J. V.; Rich, V. I.; Singh, B. K.; Stein, L. Y.; Stewart, F. J.; Sullivan, M. B.; van Oppen, M. J. H.; Weaver, S. C.; Webb, E. A.; Webster, N. S. Scientists' warning to humanity: microorganisms and climate change. *Nat. Rev. Microbiol.* **2019**, *17*, 569−586.

(4) Bossio, D. A.; Cook-Patton, S. C.; Ellis, P. W.; Fargione, J.; Sanderman, J.; Smith, S.; Wood, R. J.; Zomer, M.; von Unger, I. M.; Emmer, B. W.; Griscom, B. W. The role of soil carbon in natural climate solutions. *Nat. Sustain.* **2020**, *3*, 391−398.

(5) Goldstein, A.; Turner, W. R.; Spawn, S. A.; Anderson-Teixeira, K. J.; Cook-Patton, S.; Fargione, J.; Gibbs, H. K.; Griscom, B.; Hewson, J. H.; Howard, J. F.; Ledezma, J. C.; Page, S.; Koh, L. P.; Rockström, J.; Sanderman, J.; Hole, D. G. Protecting irrecoverable carbon in Earth's ecosystems. *Nat. Clim. Chang* . **2020**, *10*, 287−295.

(6) Woolf, D.; Amonette, J. E.; Street-Perrott, F. A.; Lehmann, J.; Joseph, S. Sustainable biochar to mitigate global climate change. *Nat. Commun.* **2010**, *1*, 56.

(7) Lehmann, J.; Hansel, C. M.; Kaiser, C.; Kleber, M.; Maher, I.; Manzoni, S.; Nunan, N.; Reichstein, M.; Schimel, J. P.; Torn, M. S.; Wieder, W. R.; Kögel-Knabner, I. Persistence of soil organic carbon caused by functional complexity. *Nat. Geosci.* **2020**, *13*, 529−534.

(8) Biochar for Environmental Management: Science, Technology and Implementation. *The Chapter: Persistence of Biochar in Soil*; Lehmann, J., Joseph, S. D., Eds., 2nd ed.; Routledge Press: London, 2015.

(9) Weng, Z.; Van Zwieten, Z.; Singh, L. V.; Tavakkoli, B. P.; Joseph, E.; Macdonald, S.; Rose, L. M.; Rose, T. J.; Kimber, M. T.; Morris, S. W. L.; Cozzolino, S.; Araujo, D.; Archanjo, J. R.; Cowie, B. S. A. C. Biochar built soil carbon over a decade by stabilizing rhizodeposits. *Nat. Clim. Chang.* **2017**, *7*, 371−376.

(10) Lehmann, J.; Cowie, A.; Masiello, C. A.; Kammann, C.; Woolf, D.; Amonette, J. E.; Cayuela, M. L.; Camps-Arbestain, M.; Whitman, T. Biochar in climate change mitigation. *Nat. Geosci.* **2021**, *14*, 883−892.

(11) Cayuela, M. L.; van Zwieten, L. V.; Singh, B. P.; Jeffery, S.; Roig, A.; Sánchez-Monedero, M. Biochar's role in mitigating soil nitrous oxide emissions: A review and meta-analysis. *Agric. Ecosyst. Environ.* **2014**, *191*, 5−16.

(12) Joseph, S.; Cowie, N.; Van Zwieten, E. R.; Bolan, Y. S.; Budai, A.; Buss, Z.; Cayuela, A. L.; Graber, L. V.; Ippolito, A.; Kuzyakov, W.; Luo, M. L.; Ok, J. A.; Palansooriya, Y.; Shepherd, Y.; Stephens, K. N.; Weng, J.; Lehmann, S.; Lehmann, J. How biochar works, and when it doesn't: A review of mechanisms controlling soil and plant responses to biochar. *GCB Bioenergy* **2021**, *13*, 1731−1764.

(13) Schmidt, H.-P.; Kammann, C.; Hagemann, N.; Leifeld, J.; Bucheli, T. D.; Sánchez Monedero, M. A. S.; Cayuela, M. L. C. Biochar in agriculture − A systematic review of 26 global meta-analyses. *GCB Bioenergy* **2021**, *13*, 1708−1730.

(14) Zamanian, K.; Pustovoytov, K.; Kuzyakov, Y. Pedogenic carbonates: forms and formation processes. *Earth-Sci. Rev.* **2016**, *157*, 1−17.

(15) Sommer, M.; Kaczorek, D.; Kuzyakov, Y.; Breuer, J. R. Silicon pools and fluxes in soils and landscapes—a review. *J. Plant Nutr. Soil* **2006**, *169*, 582.

(16) Bughio, M. A.; Wang, P. L.; Meng, F. Q.; Chen, Q.; Kuzyakov, Y.; Wang, X. J.; Junejo, S. A. Neoformation of pedogenic carbonates by irrigation and fertilization and their contribution to carbon sequestration in soil. *Geoderma* **2016**, *262*, 12−19.

(17) Beerling, D. J.; Kantzas, E. P.; Lomas, M. R.; Wade, P.; Eufrasio, R. M.; Renforth, P.; Sarkar, B.; Andrews, M. G.; James, R. H.; Pearce, C. R.; Mercure, J.-F.; Pollitt, H.; Holden, P. B.; Edwards, N. R.; Khanna, M.; Koh, L.; Quegan, S.; Pidgeon, N. F.; Janssens, I. A.; Hansen, J.; Banwart, S. A. Potential for large-scale CO_2 removal via enhanced rock weathering with croplands. *Nature* **2020**, *583*, 242−248.

(18) Lehmann, J.; Possinger, A. Removal of atmospheric CO_2 by rock weathering holds promise for mitigating climate change. *Nature* **2020**, *583*, 204−205.

(19) Service, R. F. The carbon vault. *Science* **2020**, *369*, 1156−1159.

(20) Shi, S. W. Q. Z. Y. L.; Zhang, Z. L.; Lou, Q.; Du, N.; Wang, Y. D.; Hu, A.; Wang, J. Q.; Gunina, A.; Song, J. Soil organic and inorganic carbon sequestration by consecutive biochar application: results from a decade field experiment. *Soil Use Manag.* **2021**, *37*, 95−103.

(21) Dong, X. L.; Singh, B. P.; Li, G. T.; Lin, Q. M.; Zhao, X. R. Biochar increased field soil inorganic carbon content five years after application. *Soil Tillage Res.* **2019**, *186*, 36−41.

(22) Lu, T. P.; Wang, X. J.; Du, Z. L.; Wu, L. P. Impacts of continuous biochar application on major carbon fractions in soil profile of North China Plain's cropland: in comparison with straw incorporation. *Agric. Ecosyst. Environ.* **2021**, *315*, 107445.

(23) Major, J.; Lehmann, J.; Rondon, M.; Goodale, C. Fate of soil-applied black carbon: downward migration, leaching and soil respiration. *Glob. Change Biol.* **2010**, *16*, 1366−1379.

(24) Yang, W.; Shang, J. Y.; Li, F.; Flury, M. Surface and colloid properties of biochar and implications for transport in porous media. *Crit. Rev. Environ. Sci. Technol.* **2019**, *50*, 2484−2522.

(25) Wang, Y.; Zhang, W.; Shang, J. Y.; Shen, C. Y.; Joseph, S. D. Chemical aging changed aggregation kinetics and transport of biochar colloids. *Environ. Sci. Technol.* **2019**, *53*, 8136−8146.

(26) Zamanian, K.; Zarebanadkouki, M.; Kuzyakov, Y. Nitrogen fertilization raises CO_2 efflux from soil inorganic carbon: a Global assessment. *Glob. Change Biol.* **2018**, *24*, 2810−2817.

(27) Monger, H. C.; Kraimer, R. A.; Khresat, S.; Cole, D. R.; Wang, X. J.; Wang, J. P. Sequestration of inorganic carbon in soil and groundwater. *Geology* **2015**, *43*, 375−378.

(28) Jeffery, S.; Abalos, D.; Prodana, M.; Bastos, A. C.; van Groenigen, J. W.; Verheijen, B. A.; Verheijen, F. Biochar boosts tropical but not temperate crop yields. *Environ. Res. Lett.* **2017**, *12*, 053001.

(29) Song, D.; Tang, J.; Xi, X.; Zhang, S.; Liang, X.; Zhou, W.; Wang, X. Responses of soil nutrients and microbial activities to additions of maize straw biochar and chemical fertilization in a calcareous soil. *Eur. J. Soil Biol.* **2018**, *84*, 1−10.

(30) Dong, X. L.; Singh, B. P.; Li, G. T.; Lin, Q. M. X. R.; Zhao, X. Biochar application constrained native soil organic carbon accumulation from wheat residue inputs in a long-term wheat-maize cropping system. *Agric. Ecosyst. Environ.* **2018**, *252*, 200−207.

(31) Lian, F.; Xing, B. S. Black carbon (biochar) in water/soil environments: molecular structure, sorption, stability, and potential risk. *Environ. Sci. Technol.* **2017**, *51*, 13517−13532.

https://doi.org/10.1021/acs.est.2c06419
Environ. Sci. Technol. 2023, 57, 1837−1847

(32) Kuzyakov, Y.; Subbotina, I.; Chen, H.; Bogomolova, I.; Xu, X. Black carbon decomposition and incorporation into soil microbial biomass estimated by ^{14}C labeling. *Soil Biol. Biochem.* **2009**, *41*, 210−219.
(33) Harris, D.; Horwáth, W. R.; van Kessel, C. Acid fumigation of soils to remove carbonates prior to total organic carbon or carbon-13 isotopic analysis. *Soil Sci. Soc. Am. J.* **2001**, *65*, 1853−1856.
(34) *Standard Operating Procedure for Soil Calcium Carbonate Equivalent. Volumetric Calcimeter Method Rome*; FAO, 2020.
(35) *Cation Exchange Capacity*; Rhoades, J., Ed.; ASA and SSSA: Madison, 1986.
(36) Husson, O.; Husson, B.; Brunet, A.; Babre, D.; Alary, K.; Sarthou, J.-P.; Charpentier, H.; Durand, M.; Benada, J.; Henry, M. Practical improvements in soil redox potential (Eh) measurement for characterization of soil properties. Application for comparison of conventional and conservation agriculture cropping systems. *Anal. Chim. Acta* **2016**, *906*, 98−109.
(37) *Standard Test Method for Chemical Analysis of Wood Charcoal. ASTM D1762-84*; ASTM International: West Conshohocken, 2007.
(38) Brodowski, S.; Rodionov, A.; Haumaier, L.; Glaser, B.; Amelung, W. Revised black carbon assessment using benzene polycarboxylic acids. *Org. Geochem.* **2005**, *36*, 1299−1310.
(39) Liu, Q.; Liu, B. J.; Zhang, Y. H.; Lin, Z. B.; Zhu, T. B.; Sun, R. B.; Wang, X. J.; Ma, J.; Bei, Q. C.; Liu, G.; Lin, X. W.; Xie, Z. B. Can biochar alleviate soil compaction stress on wheat growth and mitigate soil N_2O emissions? *Soil Biol. Biochem.* **2017**, *104*, 8−17.
(40) Weng, Z. H.; Van Zwieten, L.; Singh, B. P.; Kimber, S.; Morris, S.; Cowie, A.; Macdonald, L. M. Plant-biochar interactions drive the negative priming of soil organic carbon in an annual ryegrass field system. *Soil Biol. Biochem.* **2015**, *90*, 111−121.
(41) Zhang, Q. Q.; Song, Y. F.; Wu, Z.; Yan, X. Y.; Gunina, A.; Kuzyakov, Y.; Xiong, Z. Q. Effects of six-year biochar amendment on soil aggregation, crop growth, and nitrogen and phosphorus use efficiencies in a rice-wheat rotation. *J. Clean. Prod.* **2020**, *242*, 118435.
(42) Sun, T. R.; Levin, B. D. A.; Guzman, J. J. L.; Enders, A.; Muller, D. A.; Angenent, L. T.; Lehmann, J. Rapid electron transfer by the carbon matrix in natural pyrogenic carbon. *Nat. Commun.* **2017**, *8*, 14873.
(43) Hossne, G. A. J.; Méndez, N. J.; Leonett, P. F. A.; Meneses, L. J. E.; Gil, M. J. A. Maize root growth under regular water content, subjected to compaction, irrigation frequencies, and shear stress. *Rev. Fac. Nac. Agron. Medellin* **2016**, *69*, 7867−7881.
(44) Ma, Y. F.; Gao, Y. H.; Feng, Q. L. Effects of pH and temperature on $CaCO_3$ crystallization in aqueous solution with water soluble matrix of pearls. *J. Cryst. Growth* **2010**, *312*, 3165−3170.
(45) Kontrec, J.; Tomašić, N.; Matijaković Mlinarić, N. M.; Kralj, D.; Njegić Džakula, B. N. Effect of pH and type of stirring on the spontaneous precipitation of $CaCO_3$ at identical initial supersaturation, ionic strength and $a(Ca^{2+})/a(CO_3^{2-})$ ratio. *Crystals* **2021**, *11*, 1075.
(46) Johnson, M. S.; Lehmann, J.; Riha, S. J.; Krusche, A. V.; Richey, J. E.; Ometto, J. P. H. B.; Couto, E. G. CO_2 efflux from Amazonian headwater streams represents a significant fate for deep soil respiration. *Geophys. Res. Lett.* **2008**, *35*, L17401.
(47) Joseph, S. D.; Camps-Arbestain, M.; Lin, Y.; Munroe, P.; Chia, C. H.; Hook, J.; van Zwieten, L.; Kimber, S.; Cowie, A.; Singh, B. P.; Lehmann, J.; Foidl, N.; Smernik, R. J.; Amonette, J. E. An investigation into the reactions of biochar in soil. *Soil Res.* **2010**, *48*, 501−515.
(48) Bumroongsakulsawat, P.; Kelsall, G. H. Effect of solution pH on CO: formate formation rates during electrochemical reduction of aqueous CO_2 at Sn cathodes. *Electrochim. Acta* **2014**, *141*, 216−225.
(49) Kuzyakov, Y.; Shevtzova, E.; Pustovoytov, K. *Carbo*nate recrystallization in soil revealed by ^{14}C labeling: Experiment, model and significance for paleo-environmental reconstructions. *Geoderma* **2006**, *131*, 45−58.
(50) Raza, S.; Kuzyakov, Y.; Zhou, J. B. Facts to acidification−induced carbonate losses from Chinese croplands. *Glob. Change Biol.* **2021**, *27*, e7−e10.
(51) Raza, S.; Miao, M.; Wang, P. Z.; Ju, X. T.; Chen, Z. J.; Zhou, J. B.; Kuzyakov, Y. Dramatic loss of inorganic carbon by nitrogen-induced soil acidification: the past, present and future of Chinese croplands. *Glob. Change Biol.* **2020**, *26*, 3738−3751.
(52) Kendall, J. The solubility of calcium carbonate in water. *Philos. Mag.* **1912**, *23*, 958−976.
(53) Wells, R. C. The solubility of magnesium carbonate in natural waters. *J. Am. Chem. Soc.* **1915**, *37*, 1704−1707.
(54) Leifeld, J.; Fenner, S.; Müller, M. Mobility of black carbon in drained peatland soils. *Biogeosciences* **2007**, *4*, 425−432.
(55) Hagemann, N.; Joseph, S.; Schmidt, H.-P.; Kammann, C. I.; Harter, J.; Borch, T.; Young, R. B.; Varga, K.; Taherymoosavi, S.; Elliott, K. W.; McKenna, A.; Albu, M.; Mayrhofer, C.; Obst, M.; Conte, P.; Dieguez-Alonso, A. D.; Orsetti, S.; Subdiaga, E.; Behrens, S.; Kappler, A. Organic coating on biochar explains its nutrient retention and stimulation of soil fertility. *Nat. Commun.* **2017**, *8*, 1089.
(56) House, W. A.; Tutton, J. A. An Investigation of the heterogeneous nucleation of calcite. *J. Cryst. Growth* **1982**, *56*, 699−710.
(57) House, W. A. Kinetics of crystallization of calcite from calcium bicarbonate solutions. *J. Chem. Soc. Faraday Trans. I* **1981**, *77*, 341−359.
(58) Kazmlerczak, T. F.; Tomson, M. B.; Nancollas, G. H. Crystal Growth of Calcium Carbonate. A Controlled Composition Kinetic Study. *J. Phys. Chem.* **1982**, *86*, 103−107.
(59) Kitano, Y.; Hood, D. W. The Influence of organic material on the polymorphic crystallization of calcium carbonate. *Geochim. Cosmochim. Acta* **1965**, *29*, 29−41.

https://doi.org/10.1021/acs.est.2c06419
Environ. Sci. Technol. 2023, 57, 1837−1847